Metallophysics and Advanced Technologies
Металофіз. новітні технол.
Metallofiz. Noveishie Tekhnol.
2025, vol. 47, No. 10, pp. 1017–1026
https://doi.org/10.15407/mfint.47.10.1017
Reprints available directly from the publisher

PACS numbers: 68.35.Ct, 68.49.Sf, 68.60.Dv, 75.50.Vv, 75.60.Ej, 75.70.Ak, 82.80.Ms

Structure, Magnetic Properties, and Thermal Stability of Mn/Pt/NiFe Stacks

M. Yu. Barabash[*,**], R. V. Pedan[*], O. Dubikovskyi[*,***], A. V. Bodnaruk[*,****], S. M. Voloshko[*], I. O. Kruhlov[*], A. K. Orlov[*], D. S. Leonov[**], A. Kaidatzis[*****,******], and I. A. Vladymyrskyi[*]

[*]*National Technical University of Ukraine 'Igor Sikorsky Kyiv Polytechnic Institute', 37, Beresteiskyi Ave., UA-03056 Kyiv, Ukraine*
[**]*Technical Centre, N.A.S. of Ukraine, 13, Pokrovs'ka Str., UA-04070 Kyiv, Ukraine*
[***]*V. E. Lashkaryov Institute of Semiconductor Physics, N.A.S. of Ukraine, 41 Nauky Ave., UA-03028 Kyiv, Ukraine*
[****]*Institute of Physics, N.A.S. of Ukraine, 46 Nauky Ave., 03028 Kyiv, Ukraine*
[*****]*Department of Physics, University of Patras, 26504 Rio, Greece*
[******]*Institute of Nanoscience and Nanotechnology, N.C.S.R. 'Demokritos', Patr. Gregoriou E and 27 Neapoleos Str., 15310 Athens, Greece*

Corresponding author: Maksym Yuriyovych Barabash
E-mail: mbarabash@nasu.kiev.ua

Citation: M. Yu. Barabash, R. V. Pedan, O. Dubikovskyi, A. V. Bodnaruk, S. M. Voloshko, I. O. Kruhlov, A. K. Orlov, D. S. Leonov, A. Kaidatzis, and I. A. Vladymyrskyi, Structure, Magnetic Properties, and Thermal Stability of Mn/Pt/NiFe Stacks, *Metallofiz. Noveishie Tekhnol.*, **47**, No. 10: 1017–1026 (2025). DOI: 10.15407/mfint.47.10.1017

In this study, we apply an original approach to form the PtMn antiferromagnetic (AFM) phase by using the sequential deposition of Mn and Pt layers onto a heated Si/SiO_2 substrate. At the following, this AFM phase is covered by the NiFe ferromagnetic (FM) layer to achieve the AFM/FM exchange coupling prominent for spintronic applications. As shown, the thermal stability of such structure is rather limited: post-deposition annealing at a temperature close to the blocking one (400°C) results in the complete absence of the exchange-bias shift of the hysteresis loop. *Per contra*, the pronounced exchange-bias effect is observed in the stack sample with Pt/Mn layer grown on the substrate heated up to 500°C.

Key words: annealing, structure, PtMn, FeNi, magnetic properties, antiferromagnet, coercivity, layered stack.

У цьому дослідженні запропоновано оригінальний підхід до формування антиферомагнетної (АФМ) фази PtMn шляхом послідовного осадження шарів Mn і Pt на нагріту підкладинку Si/SiO_2. На наступному етапі на дану АФМ-фазу осаджено феромагнетний (ФМ) шар NiFe з метою досягнення АФМ/ФМ обмінного зв'язку, потрібного для застосування у пристроях спінтроніки. Показано, що термічна стійкість такої структури є достатньо обмеженою: відпал за температури, близької до температури блокування (400°C), призвів до повної відсутности зсуву польової залежности намагнетованости, зумовленої обмінним зв'язком. З іншого боку, виразний ефект обмінного зміщення спостерігався у зразку з шарами Pt/Mn, осадженими на підкладинку, нагріту до 500°C.

Ключові слова: відпал, структура, PtMn, FeNi, магнетні властивості, антиферомагнетик, коерцитивна сила, шарувата композиція.

(Received 2 July, 2025; in final version, 12 September, 2025)

1. INTRODUCTION

Layered stacks containing exchange-coupled ferromagnetic (FM) and antiferromagnetic (AFM) layers are of strong practical interest due to their widespread applications in modern technologies of nanoelectronics and spintronics [1]. In particular, spin-valve structures are indispensable components of magnetic sensors and information storage devices [2]. Such structures consist of two FM layers separated by a nonmagnetic one. Magnetization of the first FM layer reacts on the external field or electric current, while the second one reveals fixed magnetization (in the fields of up to several kOe) due to its strong coupling with the AFM layer and realization of the exchange bias phenomenon [3]. This effect is manifested in the shift of the hysteresis loop of the FM layer along the field axis due to spin configurational relaxation. Magnitude of this shift—exchange-bias field—decreases with temperature and vanishes at some critical temperature called the blocking temperature. Therefore, one of the main criteria determining the pos-

sibility of practical application of the AFM/FM heterostructures with exchange bias effect is their high thermal stability.

Thus, AFM materials with both high Néel and blocking temperatures are particularly relevant. In this regard, the chemically-ordered $L1_0$-MnPt phase is attractive due to its high Néel (600°C) and blocking (400°C) temperatures, pronounced AFM anisotropy ($1.4 \cdot 10^6$ J/m^3), and excellent corrosion resistance [1].

However, MnPt thin films deposited onto room-temperature substrate reveal a disordered $A1$ structure, paramagnetic properties, and no coupling with FM layers. Thermal processing of the initially disordered films or sputtering onto heated substrates is necessary to form the ordered $L1_0$-MnPt phase.

Several approaches are widely used to fabricate AFM MnPt thin films. For instance, ion beam deposition, allowing precise control over layer thickness and interface quality, followed by the post-deposition heat treatment stage, could be used for this purpose. In this regard, M. Rickart *et al.* obtained MnPt films *via* ion-beam deposition onto Si/SiO_2 substrates with a Ta buffer layer and showed that both exchange coupling with FM CoFe layer and blocking temperature reveal pronounced dependence on the post-annealing conditions [4].

Molecular beam epitaxy could be used for epitaxial growth of MnPt films, providing atomically precise chemical composition of thin-film material, excellent crystalline quality, and a possibility to tune the thickness and orientation of the film. For instance, Zhiqi Liu *et al.* formed high-quality epitaxially grown MnPt films on oxide substrates ($SrTiO_3$, $BaTiO_3$, or $MgAl_2O_4$) *via* molecular-beam epitaxy, revealing a superiorly large exchange coupling with a FM layer [5].

In addition, conventional magnetron sputter deposition followed by thermal annealing is often used to promote the $L1_0$-MnPt phase formation. In this case, a single-layer MnPt alloy film is deposited, for instance, onto glass [6, 7] or $Si(100)/SiO_2$ [8] substrates, exhibiting disordered $A1$-MnPt phase, which then transforms into the ordered $L1_0$-MnPt one upon annealing at relatively high temperatures. Such a processing route, despite its advantages, still requires optimization of deposition and heat treatment conditions in order to minimize the onset temperature of $L1_0$ ordering and to control both grain size and orientation.

Alternatively, recently, we have reported an original approach of $L1_0$-MnPt films' formation, which consisted in room-temperature deposition of Mn/Pt-based layered stacks, their following annealing in vacuum at relatively low temperatures (< 400°C) and formation of the required AFM phase *via* diffusion-driven structural transitions based on grain-boundary homogenization mechanism [9]. In particular, we have provided a quantitative estimation of diffusion coefficients under different mechanisms in Mn/Pt-based stacks with various initial

configurations of the metal layers.

It is important to note that the formation of the $L1_0$-MnPt phase governed by the grain boundary diffusion is a technologically relevant approach. It allows lowering of the processing temperature and preventing undesirable structural changes like recrystallization-induced coarsening and surface morphology degradation. Moreover, we have achieved formation of the required $L1_0$ phase without application of additional seed layers and magnetic field during films' annealing or cooling, simplifying the technological route.

Considering the high interest in the chemically ordered AFM $L1_0$-MnPt phase, its coupling with various FM layers has been widely reported. For instance, Pal and Das have recently reported the exchange-bias field of 6 mT in the annealed MnPt/Gd-based stacks, which was inversely dependent on the FM-layer thickness [10]. H. W. Chang *et al.* have investigated exchange coupling between MnPt and Co layers depending on their stacking sequence [7]. In this study, as commonly accepted, the MnPt layer has been deposited at room temperature from the alloy target and the following annealing has been performed to promote $L1_0$ ordering. It was found that the exchange bias field increases with annealing temperature due to the enhancement of the MnPt phase ordering degree. Moreover, the exchange bias field is strongly affected by the stacking of MnPt and Co layers (top or bottom position), caused by different stress/strain states of the layers. The thermal stability of AFM MnPt and IrMn layers exchange-coupled with FM CoFe layer has been investigated by Hua Lv *et al.* [11]. The authors have found that the MnPt alloy layer deposited at room temperature and subjected to the following annealing reveals a higher blocking temperature compared to the IrMn alloy after the same deposition/treatment route.

In a very recent paper by S. Isogami *et al.*, coupled $L1_0$ chemically-ordered FM FePt and AFM MnPt layers have been grown at elevated temperatures on MgO(001) single crystal substrate, evidencing the prospect of such stack application for advanced heat-assisted spin-torque magnetic recording [12].

In the present study, we applied an original approach—sequential deposition of the individual Mn and Pt layers onto a heated Si/SiO_2 substrate—to achieve MnPt alloy formation, and subsequently, a FM NiFe layer room temperature deposition on the top to investigate the magnetic behaviour of the formed AFM/FM heterostructure. We have applied different substrate temperatures (500°C and 600°C) when growing the Mn/Pt layers in order to reveal their effect on the layers' homogenization. Moreover, we investigated the thermal stability of the formed exchange-coupled AFM/FM stack at a relatively high temperature (vacuum annealing at 400°C) close to blocking one by means of analysis of the structural and magnetic properties change.

2. EXPERIMENTAL DETAILS

Layered Mn(20 nm)/Pt(24.5 nm)/NiFe(30 nm) stacks were obtained by DC magnetron sputtering (base pressure: $1 \cdot 10^{-9}$ mbar, Ar sputter pressure: $3 \cdot 10^{-3}$ mbar). Mn and Pt layers were deposited separately from pure metallic targets, at elevated temperature (500°C or 600°C) onto Si(001)/SiO_2(100 nm) substrates. After the sample holder had cooled down to the room temperature, the NiFe alloy layer was deposited at the top of the film. After that, a heat treatment of the AFM/FM stacks was performed at 400°C for 30 min in a vacuum of 10^{-6} mbar.

Chemical depth profiling of the thin films was performed using the secondary ion mass spectrometry (SIMS) technique with a primary beam of negative Cs^- (2 keV) ions at Ion Tof IV device. Phase composition of the as-deposited and post-annealed films was analysed using x-ray diffraction (XRD) in $\theta-2\theta$ geometry at Rigaku Ultima IV diffractometer equipped with CuK_α radiation source. Finally, magnetic properties ($M-H$-hysteresis loops) of the samples were investigated by vibrating sample magnetometry (VSM) at room temperature.

3. RESULTS AND DISCUSSION

Figure 1 shows the x-ray diffraction patterns of the Mn(20 nm)/Pt(24.5 nm)/NiFe(30 nm) stack after deposition at various substrate temperatures (Fig. 1, *a*, *b*) and post-annealing in a vacuum at 400°C for 30 min (Fig. 1, *c*, *d*). The pronounced diffraction peaks of PtMn(111) and PtMn(200), as well as FeNi(111), are clearly seen in the XRD patterns of the as-deposited films regardless of the deposition temperature (Fig. 1, *a*, *b*). These results confirm that elevated temperatures used for Pt and Mn layers deposition are enough for activation of diffusion interaction between these elements and formation of PtMn alloy. It should be noted that no noticeable effect of the substrate temperature on the angle position and intensity of the mentioned diffraction peaks was detected. PtMn alloy exhibits a disordered cubic crystal structure in the as-deposited state, which is evidenced by the absence of superlattice peaks. This indicates that despite a relatively high substrate temperature, just heating the substrate is not enough for chemical ordering of the PtMn alloy.

Figure 2 shows the SIMS chemical depth profiles of the investigated Mn(20 nm)/Pt(24.5 nm)/NiFe(30 nm) stacks after deposition at various substrate temperatures and post-annealing in a vacuum at 400°C for 30 min. These data are displayed as secondary ions emission intensity as a function of sputtering time, which is related to the film depth. As can be seen, there are relatively sharp interfaces between the top FeNi and bottom PtMn layers in the as-deposited samples (Fig. 2, *a*, *b*). At the same time, Mn and Pt are already intermixed in the as-deposited

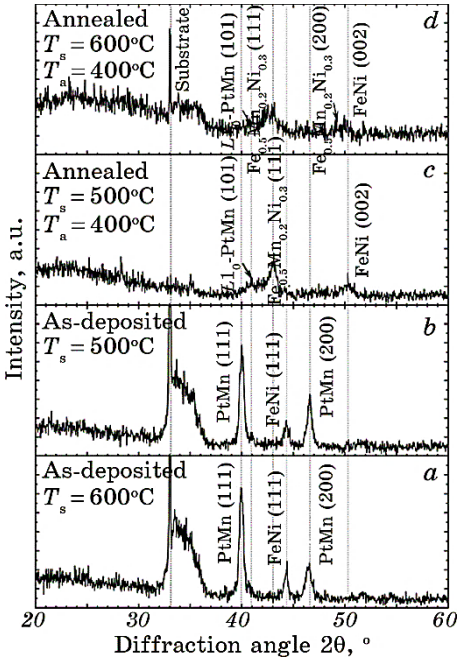

Fig. 1. XRD patterns of the sub/Mn(20 nm)/Pt(24.5 nm)/NiFe(30 nm) stack after deposition at various substrate temperatures and post-annealing in a vacuum at 400°C for 30 min.

samples that is well agreed with XRD data and is related to the formation of the relatively homogeneous PtMn-alloy layer.

In addition, it should be noted that the distribution of Ni and Fe through the top NiFe layer is fully homogeneous. An increase in the substrate temperature during deposition of Pt and Mn layers up to 600°C results in more uniform Pt distribution, while deposition at 500°C results in increased Pt concentration at the near-substrate region.

Annealing in vacuum at 400°C of the Mn(20 nm)/Pt(24.5 nm)/NiFe(30 nm) stack leads to formation of the ternary $Fe_{0.5}Mn_{0.2}Ni_{0.3}$ compound with a face-centred crystal structure and $L1_0$ ordering of the PtMn alloy, resulting in tetragonal distortion of its lattice (Fig. 1, *c*, *d*). Moreover, heat treatment leads to the whole homogenization of Pt, Fe, and Ni, as well as close-to-homogeneous spatial distribution of Mn through the film depth (Fig. 2, *c*, *d*). This indicates that the phase composition and distribution of the chemical elements of the formed stacks are not stable under temperatures close to the blocking one. Moreover, higher temperature of Pt/Mn layer deposition (600°C) leads to more uniform Mn distribution through the depth of the post-annealed stack.

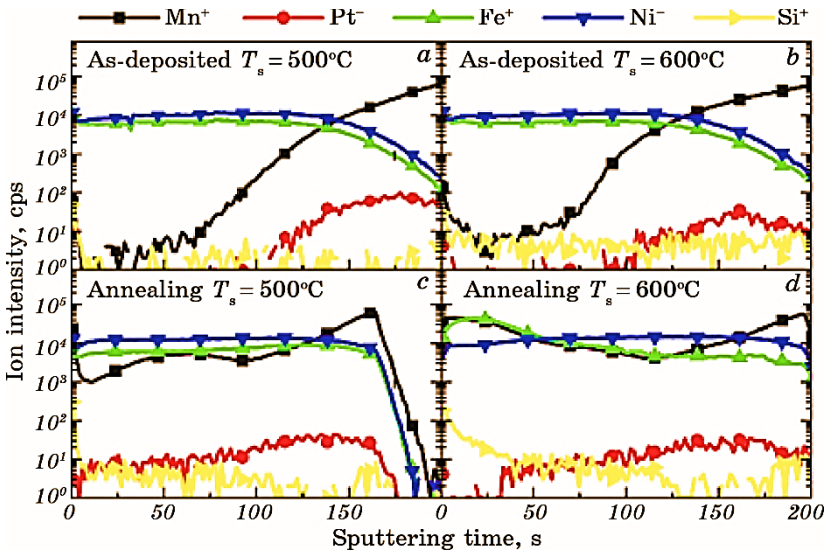

Fig. 2. SIMS chemical depth profiles of the sub/Mn(20 nm)/Pt(24.5 nm)/NiFe(30 nm) stack after deposition at various substrate temperatures and annealing at 400°C for 30 min.

Figure 3 shows the VSM M–H-hysteresis loops of the Mn(20 nm)/Pt(24.5 nm)/NiFe(30 nm) stacks deposited at various temperatures and subjected to the following annealing in vacuum. As can be seen in Fig. 3, *a*, the only case when the exchange-bias shift of the hysteresis loop is observed (in the magnetic field applied perpendicular to the film plane) is the sample deposited at 500°C. The value of this shift is 103 Oe in the direction of the positive field. Notably, this bias shift is not detected anymore after post-annealing of the sample. Furthermore, there is no exchange-bias shift for either the as-prepared stack deposited at higher substrate temperature, or the post-annealed stacks.

The in-plane magnetic anisotropy is typical for all investigated cases—magnetization is much higher in the case of the external field applied parallel to the film surface compared to a perpendicular one. This is quite common for thin films, exhibiting an easy magnetization axis that lies in the film plane. For the as-deposited samples, coercivity is higher for a perpendicularly applied field. At the same time, as has already been mentioned above, the post-annealing process leads to the vanishing of the exchange-bias shift. Moreover, post-annealed samples revealed lower magnetization and higher coercivity measured in the parallel field. As follows from the analysis of XRD and SIMS data, such annealing-induced changes in magnetic behaviour are attributed to drastic modification of the phase composition and elemental redis-

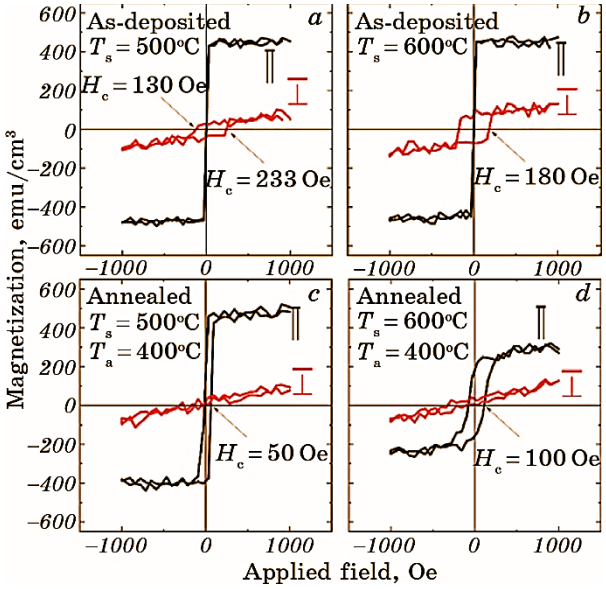

Fig. 3. VSM M–H-hysteresis loops of sub/Mn(20 nm)/Pt(24.5 nm)/NiFe(30 nm) stack after deposition at various substrate temperatures and post-annealing in a vacuum at 400°C for 30 min.

tribution as a result of heat treatment.

Magnetic characterization data indicate that the only sample demonstrating the exchange-bias shift among all thin films under study is the one deposited on the substrate heated to 500°C (Fig. 3, *a*). According to the SIMS depth profiling data (Fig. 2, *a*), this is the only sample where no diffusion of either Mn or Pt to the ferromagnetic NiFe layer is detected. Therefore, the integrity of the FM/AFM interface, when the diffusion intermixing between the AFM and FM materials is frozen, is crucial for the realization of the exchange bias phenomenon. When the substrate is heated to a higher temperature (600°C), the Mn-atoms' diffusion into the FeNi layer becomes more pronounced (Fig. 2, *b*), which eliminates the exchange bias (Fig. 3, *b*). Similarly, in both post-deposition annealed stacks, the FM/AFM interfaces are blurred (Fig. 2, *c*, *d*) due to the intensive diffusion of both Pt and Mn atoms towards the upper FeNi layer. Furthermore, higher substrate temperature as well as the post-annealing should negatively affect both the grain size and the interfacial roughness between metal layers, which can also contribute to the disappearance of the exchange bias shift.

Another point which is worth noting is that the exchange bias is observed in the sample, which, according to the XRD data (Fig. 1, *a*), is characterized by the disordered PtMn structure. As has already been mentioned, typically, the exchange bias is realized in the presence of

the chemically ordered $L1_0$ ferromagnetic phase. Therefore, it is most likely that the PtMn phase formed upon deposition of the initially layered stack at 500°C is characterized by a short-range ordering, which cannot be detected by XRD. Short-range ordering is not particularly new in thin films, for instance, it has already been observed in Pt/Co stacks upon annealing above 400°C [13].

It is also noticeable that the exchange bias disappears (Fig. 3, *c*) upon post-annealing of the sample deposited at 500°C, despite the corresponding XRD data showing the annealing-induced formation of the $L1_0$-ordered phase. It is likely that the ordered phase formed during post-annealing is distributed in the film volume, not as a single layer but rather as island-type inclusions, which would not yield the exchange bias with the FM layer.

4. CONCLUSION

Thin films composed of exchange-coupled ferromagnetic (FM) and antiferromagnetic (AFM) layers are of high application interest due to their widespread use in magnetic sensors and magnetic storage devices. In this study, we intended to explore the thermal stability of the structural and magnetic characteristics of the AFM/FM structure, consisting of MnPt (AFM) and FeNi (FM) layers. For this purpose, we applied the following steps: (i) sequential deposition of the Mn and Pt layers onto a heated up to 500°C and 600°C Si/SiO_2 substrate, which was followed by (ii) the room-temperature deposition of the top NiFe layer, and then, (iii) vacuum post-annealing at 400°C for 30 min. As has been shown by means of the structural analysis and chemical depth profiling, regardless of the deposition temperature, the as-received stacks are characterized by the disordered MnPt structure covered by the homogeneous FeNi layer. However, the significant effect of substrate temperature has been found in the magnetic properties' behaviour: the only sample demonstrated pronounced exchange-bias effect in the perpendicular magnetic field was the one sputtered at 500°C, whereas the post-annealing resulted in the loss of this effect. Nevertheless, it is notably that the samples subjected to post-growth annealing revealed an increased coercivity in the parallel magnetic field, indicating the temperature-induced change of the magnetic behaviour.

The work was supported by the Ministry of Education and Science of Ukraine (projects 0123U101257 and 0124U001266).

REFERENCES

1. A. Hafarov, O. Prokopenko, S. Sidorenko, D. Makarov, and I. Vladymyrskyi, *Conf. Proc. 'Modern Magnetic and Spintronic Materials' NATO Science for*

Peace and Security Series B: Physics and Biophysics (Eds. A. Kaidatzis, S. Sidorenko, I. Vladymyrskyi, and D. Niarchos) (Dordrecht: Springer: 2020), p. 73.
2. J. M. Teixeira, J. Ventura, J. P. Araujo, J. B. Sousa, V. S. Amaral, B. Negulescu, M. Rickart, and P. P. Freitas, *J. Non-Crystalline Solids*, **354**, Iss. 47–51: 5275 (2008).
3. R. Y. Umetsu, C. Mitsumata, A. Sakuma, and K. Fukamichi, *Tran. Magn. Society of Japan*, **3**, Iss. 3: 59 (2003).
4. M. Rickart, P. P. Freitas, I. G. Trindade, N. P. Barradas, E. Alves, M. Salgueiro, N. Muga, J. Ventura, J. B. Sousa, G. Proudfoot, D. Pearson, and M. Davis, *J. Appl. Phys.*, **95**: 6317 (2004).
5. Z. Liu, M. D. Biegalski, S.-L. Hsu, S. Shang, C. Marker, J. Liu, L. Li, L. Fan, T. L. Meyer, A. T. Wong, J. A. Nichols, D. Chen, L. You, Z. Chen, K. Wang, K. Wang, T. Z. Ward, Z. Gai, H. N. Lee, A. S. Sefat, V. Lauter, Z.-K. Liu, and H. M. Christen, *Adv. Mater.*, **28**, Iss. 1: 118 (2015).
6. S. Honda, M. Nawate, and T. Norikane, *J. Magn. Magn. Mater.*, **220**, Iss. 1: 85 (2000).
7. C. W. Chang, F. T. Yuan, P. Y. Yeh, Y. C. Chen, Y. L. Lai, P. H. Pan, C. R. Wang, L. Horng, and W. C. Chang, *AIP Advances*, **9**, Iss. 3: 035330 (2019).
8. H. W. Chang, C. Y. Shen F. T. Yuan, P. H. Pan Y. H. Chien, C. R. Wang, L. Horng, and S. R. Jian, *Thin Solid Films*, **660**: 834 (2018).
9. S. M. Voloshko, I. O. Kruhlov, R. Pedan, M. Garrido-Segovia, A. Orlov, O. Dubikovskyi, J. M. Garcia-Martin, A. Kaidatzis, and I. A. Vladymyrskyi, *Phys. Scripta*, **99**: 115973 (2024).
10. K. Pal and I. Das, *Thin Solid Films*, **790**: 140211 (2024).
11. H. Lv, D. C. Leitao, K. Pruegl, W. Raberg, P. P. Freitas, and S. Cardoso, *J. Magn. Magn. Mater.*, **477**: 68 (2019).
12. S. Isogami, Y. Sasaki, Y. Fan, Y. Kubota, J. Gadbois, K. Hono, and Y. K. Takahashi, *Acta Mater.*, **286**: 120743 (2025).
13. R. Pedan, P.Makushko, O. Dubikovskyi, A. Bodnaruk, A. Burmak, S. Sidorenko, S. Voloshko, V. Kalita, R. Hübner, and D. Makarov, *J. Phys. D: Appl. Phys.*, **55**, No. 40: 405004 (2022).